HIGH-RESOLUTION OPTICAL MICROSCOPY OF $Ba_XSr_{1-X}TiO_3$ FILMS

C. HUBERT*, J. LEVY*, A. C. CARTER**, W. CHANG**, J. M. POND**, J.S. HORWITZ**, D. B. CHRISEY**
*Dept. of Physics, University of Pittsburgh, Pittsburgh, PA 15260, jlevy@pitt.edu
** Naval Research Laboratory, Washington, D.C. 20375

ABSTRACT

The ferroelectric polarization of thin films of $Ba_xSr_{1-x}TiO_3$ is imaged using confocal scanning optical microscopy (CSOM). The thin films are grown by pulsed laser deposition (PLD) on $SrTiO_3$ substrates. Ferroelectric domain structure is imaged by applying a small ac electric field across interdigitated electrodes, and measuring induced reflectivity changes in the film, which are directly related to the polarization. Domain re-orientation is observed by acquiring CSOM images as a function of the dc electric field. Local hysteresis loops are obtained by sweeping the dc electric field at fixed positions on the sample. Micrometer-sized regions exhibit both ferroelectric and paraelectric response, indicating that thermal broadening of the phase transition is largely due to inhomogeneities in the thin films.

INTRODUCTION

Ferroelectrics are promising materials for the development of frequency-agile microwave electronics [1-4]. The principal obstacle to their use is the relatively high dielectric loss at microwave frequencies, which is orders of magnitude larger than for bulk materials.

Optical methods can provide important clues to the mechanisms for dielectric loss over relevant micrometer and nanometer length scales. A technique based on confocal scanning optical microscopy (CSOM) has been developed for probing ferroelectric domain structure and dynamics by measuring small polarization-induced changes in the refractive index [5]. The high sensitivity ($\Delta n/n \sim 10^{-7}$) and high spatial resolution of this technique (<0.5 μm) could help to identify factors contributing to dielectric loss, such as grain boundaries and other structural imperfections, domain wall dynamics, non-uniform strain, and variations in stoichiometry.

EXPERIMENT

Thin films (~3500 Å thick) of $Ba_xSr_{1-x}TiO_3$ (x=0.5,0.8) are grown on (100) $SrTiO_3$ substrates by pulsed laser deposition (PLD) as previously described [6] and characterized by X-ray diffraction (XRD) and scanning electron microscopy (SEM) [6]. As-deposited films are single phase and (100) oriented. The as-deposited films show grain sizes ranging from 50-200 nm, depending on the composition x. Annealing at temperatures ≤ 1250 °C in flowing oxygen improves both the structural and dielectric properties of the deposited film [7]. Post-

Mat. Res. Soc. Symp. Proc. Vol. 493 © 1998 Materials Research Society

annealed films exhibit lower dielectric loss and reduced non-uniform strain due to an increase in the overall grain size and filling of oxygen vacancies [7]. The optical and dielectric properties of the $Ba_xSr_{1-x}TiO_3$ ferroelectric films are characterized using interdigitated capacitors. The structures are patterned from e-beam evaporated silver films deposited through a liftoff mask on top of an $Ba_xSr_{1-x}TiO_3$ film. To minimize metal losses at microwave frequencies, the metal is several skin depths thick (~3 μm). In the interdigitated structure, the distance between electrodes is 7.5-15 μm. When the film is biased, the electric field lines point along the (010) direction. The temperature and electric field dependence of the dielectric properties have been measured at 1 MHz and the field dependence has been measured at room temperature from 1 - 20 GHz, and are described elsewhere [3,8].

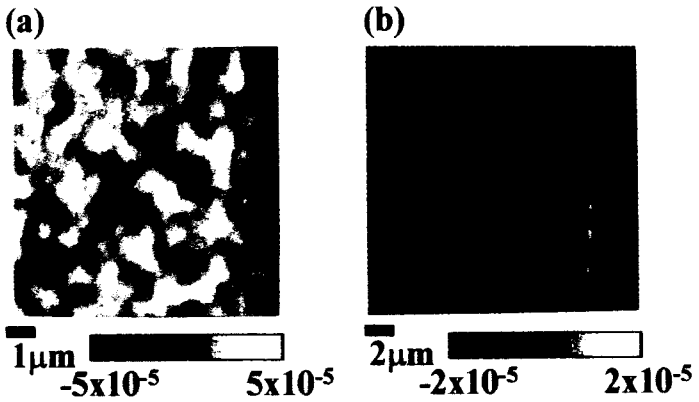

Figure 1. CSOM images of two thin films taken at zero bias. (a) $Ba_{0.8}Sr_{0.2}TiO_3$ film deposited on (100) $SrTiO_3$ and (b) $SrTiO_3$ film deposited on (100) $SrTiO_3$. No signal is observed for the $SrTiO_3$ film since it is in the paraelectric (cubic) phase.

The CSOM experimental setup is as follows: a linearly polarized Helium-Neon laser (λ=633 nm) is focused to a diffraction-limited spot (~470 nm diameter) on the film surface. A combined dc and ac electric field is applied to the film *via* the interdigital electrodes on the sample ($E(t) = E_{dc} + E_{ac}\cos(\omega t)$, $\omega/2\pi$=50 kHz). Electric field-induced reflectivity changes in the thin film arise from the linear electro-optic effect, the coefficient of which is proportional to the spontaneous ferroelectric polarization P_s [9]. The reflected light intensity r is modulated at the frequency of the driving field, and detected with a lock-in amplifier. This lock-in signal dr/dE is normalized by r to form the CSOM signal. All measurements are performed at ambient room temperature (~295 K).

Measurements are performed in two modes. In one mode, images of the ferroelectric polarization are obtained by raster-scanning the sample at a fixed dc electric field. In this way, it is possible to track the re-orientation of ferroelectric domains as a function of the applied field. In the second mode, the dc electric field is slowly swept while acquiring data at a fixed point on the sample. These traces yield information about the local hysteretic behavior of the sample.

RESULTS

CSOM images of two different thin films are shown in Figure 1. Figure 1(a) shows an image of a $Ba_{0.8}Sr_{0.2}TiO_3$ film deposited on $SrTiO_3$ taken at E_{dc}=0 kV/cm. On the rightmost side of the image is one of the interdigitated electrodes. Polarization fluctuations are evident across the entire sample. By comparison, a $SrTiO_3$ film grown on $SrTiO_3$, shows no signal at all, since the film is paraelectric.

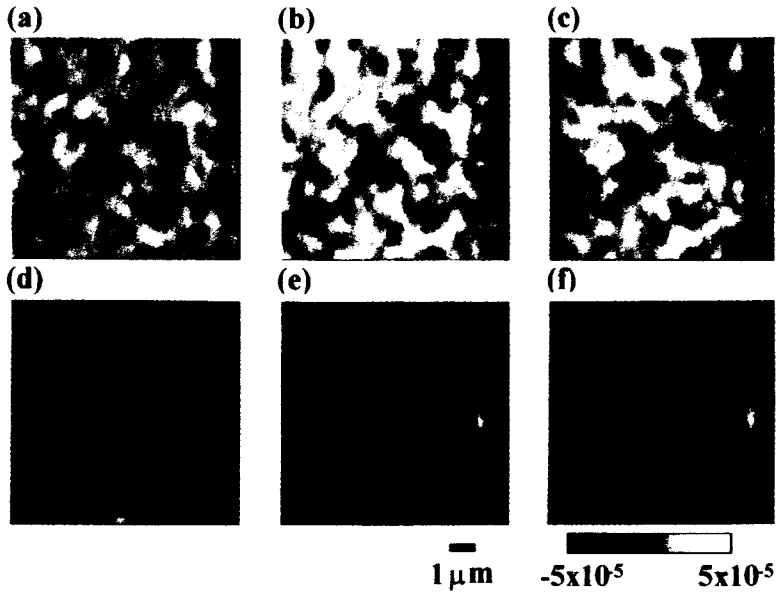

Figure 2. CSOM images of the same as-deposited $Ba_{0.8}Sr_{0.2}TiO_3$ sample shown in Fig. 1(a), taken at different dc biases. Images (a)-(c) are taken at increasing dc biases (a) -4 kV/cm, (b) 0 kV/cm, (c) 4 kV/cm. Images (d)-(f) were obtained in the reverse order presented: (d) -4 kV/cm, (e) 0 kV/cm, (f) 4 kV/cm. Note that upper and lower images were taken at the same dc bias but with different histories. Several regions (*e.g.*, upper right corner) show domains that have completely reversed their orientation.

Figure 2 illustrates the history dependence of the ferroelectric polarization as the dc electric field is slowly varied. Figures 2(a-c) show images taken at increasing dc electric fields. There is an overall decrease in the signal as the field is increased, corresponding to the change in the average polarization. However, the fluctuations are large and field-dependent. A comparison of Figures 2(a) and 2(c) shows several regions which have reversed their orientation at low fields. Figures 2(d-f) show successive images taken at decreasing dc electric fields. A comparison between upper and lower images (*e.g.* (b) and (e)) indicates significant hysteresis.

Figure 3 shows hysteresis loops taken for two $Ba_{0.5}Sr_{0.5}TiO_3$ samples grown from different targets. Both samples were annealed in O_2 at 1250 °C. Figures 3(a-b) shows hysteresis loops for the first film, taken at two regions that are separated by less than 1 μm. While Fig. 3(a) shows clear hysteresis, the neighboring region (Fig. 3(b)) exhibits a much smaller response with no hysteresis. These variations are attributed to local fluctuations in the Curie temperature of the film, *i.e.*, T<Tc for Fig. 3(a), and T>Tc for Fig. 3(b). Figs. 3(c-d) shows similar variations in regions which are separated by microns. The double hysteresis loop seen in Fig. 3(c) is expected at temperatures just above a first-order phase transition [10], although such behavior may also arise due to polarizable defects [10]. The orientation of hysteresis loops is also found to vary at different parts of the sample, as seen in Fig. 3(d). Such complicated shapes are commonly observed, and are believed to result from interactions between neighboring domains.

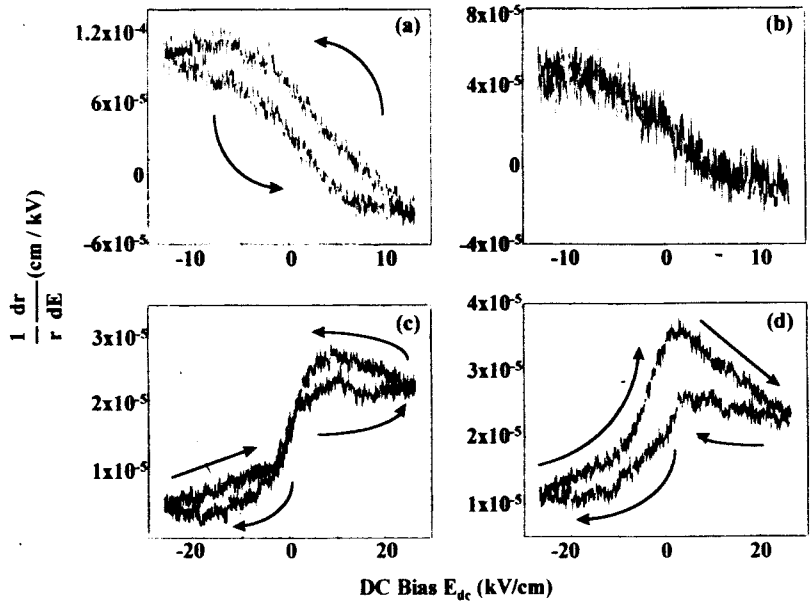

Figure 3. Optically measured hysteresis loops from thin film samples: (a) and (b) are from a $Ba_{0.5}Sr_{0.5}TiO_3$ sample compensated with 2% Sr and "bomb" annealed, (c) and (d) are from a sample of $Ba_{0.5}Sr_{0.5}TiO_3$ which was only annealed. Both films were grown on $SrTiO_3$.

CONCLUSIONS

In many respects, the thin films grown on $SrTiO_3$ exhibit behavior which is closer to the bulk single crystals, showing higher dielectric constants, a more sharply peaked temperature dependence, and lower dielectric losses [8]. X-ray ω-scans for the (002) peaks were on the order of 0.1 -0.2° FWHM for films deposited on $SrTiO_3$. Nevertheless, the phase transition T_c is still sufficiently broad that ferroelectric switching is observed in nominally paraelectric (x=0.5) films. The most likely source of the broadened transition temperature is non-uniform stress. Uniaxial [11] and two-dimensional [12] stress shift the Curie point to higher temperatures, while hydrostatic stress has the opposite effect [13]. In bulk $BaTiO_3$, the dielectric loss tanδ(T) at 24 GHz is sharply peaked just below the Curie temperature [14]. An inhomogeneous shifting of T_c would give rise to micro-regions in which the dielectric loss was quite large. Measurements performed as a function of temperature will help to confirm this. Higher resolution optical probes such as near-field scanning optical microscopy [15,16] may also help shed light on the nanometer domain orientation and dynamics and their contribution to dielectric loss in ferroelectric thin films.

ACKNOWLEDGEMENTS

Support from a National Science Foundation CAREER award (J.L.) and the Office of Naval Research is gratefully acknowledged.

REFERENCES

1. V. K. Varadan, D. K. Ghodgaonkar, V. V. Varadan, J. F. Kelly, and P. Glikerdas, Microwave Journal **35,** 116, 119, 121-2, 125, 127 (1992).

2. R. W. Babbitt, T. E. Koscica, and W. C. Drach, Microwave Journal **35,** 63-4, 69, 71, 73, 76-9 (1992).

3. K. R. Carroll, J. M. Pond, D. B. Chrisey, J. S. Horwitz, R. E. Leuchtner, and K. S. Grabowski, Appl. Phys. Lett. **62,** 1845-7 (1993).

4. J. S. Horwitz, D. B. Chrisey, J. M. Pond, R. C. Y. Auyeung, C. M. Cotell, K. S. Grabowski, P. C. Dorsey, and M. S. Kluskens, Integrated Ferroelectrics **8,** 53-64 (1995).

5. C. Hubert, J. Levy, A. C. Carter, W. Chang, J. M. Pond, J. S. Horwitz, and D. B. Chrisey, to appear in Appl. Phys. Lett. **71,** Dec. 8 issue (1997).

6. S. B. Qadri, J. S. Horwitz, D. B. Chrisey, R. C. Y. Auyeung, and K. S. Grabowski, Appl. Phys. Lett. **66,** 1605-7 (1995).

7. L. A. Knauss, J. M. Pond, J. S. Horwitz, D. B. Chrisey, C. H. Mueller, and R. Treece, Appl. Phys. Lett. **69,** 25-7 (1996).

8. J. S. Horwitz, D. B. Chrisey, A. C. Carter, W. Chang, L. A. Knauss, J. M. Pond, S. K. Kirchoefer, D. Korn, and S. B. Qadri, Proc. SPIE **2991,** 238 (1997).

9. W. J. Merz, Phys. Rev. **76,** 1221-5 (1949).

10. M. E. Lines and A. M. Glass, *Principles and Applications of Ferroelectrics and Related Materials* (Clarendon, Oxford, 1977).

11. A. Aharony and A. D. Bruce, Physical Review Letters **33,** 427-30 (1974).

12. G. A. Rosetti, Jr., L. E. Cross, and K. Kushida, Applied Physics Letters **59,** 2524-6 (1991).

13. G. A. Rossetti, Jr., K. R. Udayakumar, M. J. Haun, and L. E. Cross, Journal of the American Ceramic Society **73,** 3334-8 (1990).

14. T. S. Benedict and J. L. Durand, Phys. Rev. **109,** 1091 (1958).

15. E. Betzig, J. K. Trautman, T. D. Harris, J. S. Weiner, and R. L. Kostelak, Science **251,** 1468-70 (1991).

16. F. Zenhausern, Y. Martin, and H. K. Wickramasinghe, Science **269,** 1083-5 (1995).